climate

MDPI

Article

Evaluating Vegetation Growing Season Changes in Northeastern China by Using GIMMS LAI3g Data

Xiliang Ni [1,†], Jianfeng Xie [2,*,†], Yuke Zhou [3], Xizhang Gao [4] and Lin Ding [1]

1 State Key Laboratory of Remote Sensing Science, Institute of Remote Sensing and Digital Earth, Chinese Academy of Sciences, Beijing 100101, China; nixl@radi.ac.cn (X.N.); dinglin@radi.ac.cn (L.D.)
2 Environmental Monitoring Center of Hebei Province, Shijiazhuang 050037, China
3 Key Laboratory of Ecosystem Network Observation and Modeling, Institute of Geographical Sciences and Natural Resources Research, Chinese Academy of Sciences, Beijing 100101, China; zhouyk@igsnrr.ac.cn
4 State Key Laboratory of Resources and Environmental Information System, Institute of Geographical Sciences and Natural Resources Research, Chinese Academy of Sciences, Beijing 100101, China; gaoxz@lreis.ac.cn
* Correspondence: xiejianfeng8007@sina.com; Tel.: +86-311-89253303
† These authors contributed equally to this work.

Academic Editor: Maoyi Huang
Received: 29 November 2016; Accepted: 17 May 2017; Published: 22 May 2017

Abstract: Accurate understanding and detecting of vegetation growth change is essential for providing suitable management strategies for ecosystems. Several studies using satellite based vegetation indices have demonstrated changes of vegetation growth and phenology. Temperature is considered a major determinant of vegetation phenology. To accurately detect the response of vegetation to climate variations, this study investigated the vegetation phenology in the northeast (NE) region of China by using in-situ temperature observations and satellite-based leaf area index estimates (LAI3g) for the period 1982–2011. Firstly, a spatial distribution of the averaged phenology over the 30 years was obtained. This distribution showed that a tendency for an early start of the growing season (SoS) and late end of the growing season (EoS) was observed towards of the southeastern part of NE China, with the late SoS and early EoS occurring at higher latitudes. Secondly, the temperature-based and satellite-based phenological trends were analyzed. Then the significant advanced trend (SAT), significant delayed trend (SDT), and nonsignificant trend (NT) of SOS and EOS in NE region of China were detected by using the Mann-Kendall trend test approach. Finally, changes in phenological trends were investigated by using the temperature-based and satellite-based phenology method. A comparison of the phenological trend shows that there are some significant advanced trends of SOS and significant delayed trends of EOS in the NE region of China over 30 years. The results of this study can provide important support of the view that a lengthening of growing season duration occurred at the northern high latitudes in recent decades.

Keywords: vegetation growth; vegetation phenology; start of the growing season (SOS); end of the growing season (EOS); China Meteorological Data (CMD); significant advanced trend (SAT); significant delayed trend (SDT); nonsignificant trend (NT); Global Inventory Monitoring and Modeling Studies Leaf Area Index third-generation (GIMMS LAI3g)

1. Introduction

During the past few decades, the ongoing climate change has had serious effects on vegetation dynamics [1–5]. Vegetation phenology, the annual rhythm of biological phenomena, is a significant indicator of climate change. The extension of the vegetation growing season could be attributed to climate changes across the globe [6–8].

Many previous studies [5–7,9–13] based on satellite phenology have demonstrated the efficiency of satellite derived indices on climatic and ecological changes in large scale. On the account of the long term, large scale, and continuous observations, most of the studies were based on long time series vegetation index datasets [10,11]. Naturally, many of these studies used the phenology metrics derived from temporally smoothed vegetation index data, such as Normalized Difference Vegetation Index (NDVI), Enhanced Vegetation Index (EVI), and Leaf Area Index (LAI). Different approaches have been identified to derive these metrics in a robust fashion [9–11,14–18]. Recent studies have also demonstrated that the uncertainty in the estimation of phenological metrics has a direct relation to the cloud contamination and the quality of satellite data [19–21]. However, the quality and research applicability of the Global Inventory Monitoring and Modeling Studies Leaf Area Index third-generation (GIMMS LAI3g) dataset were effectively evaluated and widely used in numerous research studies [22–25], which indicated that LAI3g data could be effectively used for deriving phenology. The phenological metrics of onset and cessation provide great insights into the effect of natural and anthropogenic factors on vegetation.

Northeast China possesses the largest contiguous forest land area in China. Northeast China has a forested land area of 50.5 million ha, which accounts for about 28.9% of China's forested land area. Northeast China is not only an important national base for wood and food products, but also plays a key role for providing various ecological services. In keeping with overarching trends in global climate change, increasing trends in mean annual temperature have been observed in Northeast China since the 1980s [26]. Therefore, the investigation of vegetation phenological changes and climate change is necessary to improve sustainable management of Northeast China's ecosystems. However, less attention has been paid to vegetation change and its relationship with climatic factors over this regional scale area [11,25–28]. As a result, some aspects of vegetation dynamics still remain poorly understood [25].

Our primary objective in this study is to detect vegetation phenology trends in Northeast China from 1982 to 2012. In the subsequent sections of this paper, we firstly describe the satellite data used in our study, and our methodology for deriving phenology, the trend test and analysis metrics. In Section 3, we present the differences between phenology metrics derived from temperatures measured in meteorological stations and the metrics derived from LAI3g dataset data. In addition, the trends in vegetation phenology across Northeast China from 1982–2011 are examined, and the spatial distribution of phenology and regional phenology trend are analyzed, which is important to understand phenology of vegetation and climate change. Finally, we discuss the observed differences between the trends derived from two metrics, and the limitation of the study is also analyzed. Due to lack of detailed analysis on precipitation and land use, the phenology model did not include precipitation and land use in the simulation for this study. Their potential influence on vegetation phenology needs to be investigated in future phonological models.

2. Materials and Methods

2.1. Study Area

The research area of this study is the Northeast region of China, which extends longitudinally from 73°24′ E to 97°00′ E and latitudinally from 34°50′ N to 49°15′ N, with a total area of 1.52×10^6 square kilometers (Figure 1). This study area covers Liaoning (LN), Jilin (JL), and Heilongjiang (HLJ) provinces and four leagues (an administrative division of the Inner Mongolia Autonomous Region) in eastern Inner Mongolia Autonomous region (IMA). The precipitation in this area generally ranges from 300 mm to 1000 mm owing to monsoon climate of medium latitudes.

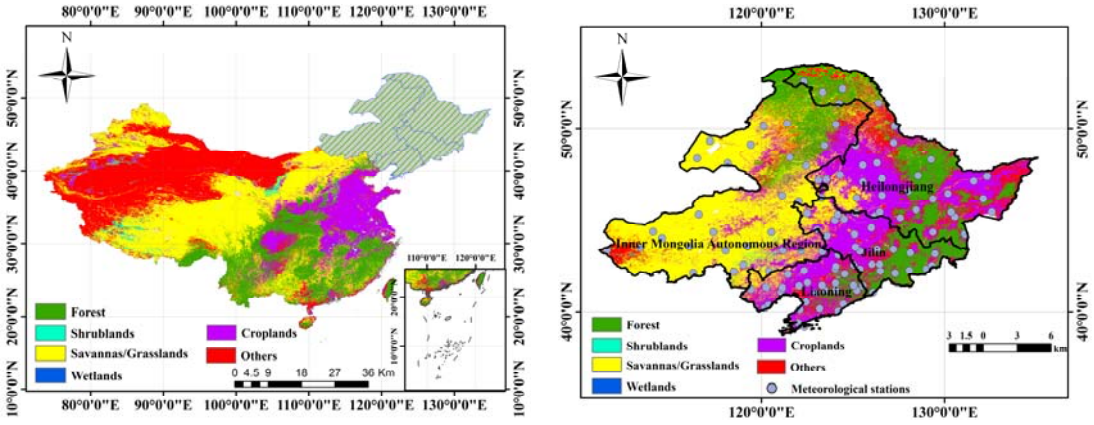

(**a**) (**b**)

Figure 1. The research area of this study. (**a**) Location of the study area in China, showing a land cover map of China. The grey region is the location of this study area. (**b**) The vegetation of the study area is separately represented by five colors. The grey circles are the distribution of meteorological stations in Northeast (NE) China.

2.2. *Datasets*

2.2.1. LAI Dataset

The LAI dataset used in this study is LAI3g, which is derived based on the third-generation NDVI (NDVI3g) [22–24], from the Advanced Very High Resolution Radiometer (AVHRR) carried by the National Oceanic and Atmospheric Administration (NOAA), produced by the Global Inventory Monitoring and Modeling Studies (GIMMS), at a spatial resolution of 1/12 degree (about 8 km) and 15-day interval, spanning from January 1982 to December 2011 [29].

2.2.2. Climate Data

The climatic variables used in this study mainly include precipitation and temperature, from China Meteorological Data Sharing Service System (CMDSSS), which include hourly and daily meteorological records observed from 754 benchmark surface weather stations and automatic weather station since 1951 [30–32]. The accuracy of these meteorological station data has been found to be over 99.9%.

Out of these 754 stations, 118 are in the area considered for this study. For the purpose of this study, only meteorological observations from 1982 to 2011 are considered.

2.2.3. Land Cover Data

For this study, we also used the IGBP (International Geosphere-Biosphere Programme) Land Cover (LC) product (MCD12Q1, 500 m) over NE China for the year 2011 [33]. The LC IGBP product used in this study area includes 11 natural vegetation classes, three developed and mosaicked land classes, and three non-vegetated land classes.

In this study, we rescaled the MCD12Q1 LC IGBP data and made its spatial resolution the same as LAI3g data by using the following statistical method [22]. We counted the classification type of MCD12Q1 LC IGBP in one pixel of LAI3g. The MCD12Q1 LC class with the largest quantity was set as a new classification type of LC resample. Based on the new LC map, which had the same scale as theLAI3g data, we selected the vegetation area to do the examination and analysis of vegetation phenology trends.

2.3. Methods

2.3.1. Phenology Metrics from Traditional Thermal Method

Numerous phenological studies consider air temperature as the key triggering factor of vegetation phenology [34,35]. The start of the growing season (SOS) and the end of the growing season (EOS) were defined according to the air temperature's change. According to these methods, the starting day of a period including five continuous days with average temperature greater than 5 degrees Celsius, is considered the SOS.

Similarly, the ending day of a period including five continuous days with average temperature greater than 5 degrees Celsius was defined as the EOS [35]. As temperature is the key factor in determining vegetation phenology, a lot of studies have used temperature based phonological metrics to detect the vegetation phenology [34–37]. Phenology metrics based upon a traditional thermal method were introduced in this study. Based on the definitions of the SOS and EOS above, the daily temperature data from meteorological observation in NE China was used to determine the phenology over the meteorological stations scale.

2.3.2. Phenology Metrics Derived from Vegetation Index

The growing season is the most active period in the phenology cycle of non-evergreen vegetation [36]. Generally, there are some different threshold methods which can be used to detect phenology, including the absolute threshold, the dynamic ratio threshold, and the abrupt change method [35]. Due to wide use of the dynamic ratio threshold method in detecting phenology recently [37–44], we used the leaf area index changes ratios to determine the onset dates of vegetation grow up and dormancy. On account of growth stages with high activity, the vegetation index in the growing season can be considered a better expressional character than the total year's vegetation index. Figure 2 shows the approach flowchart of this study.

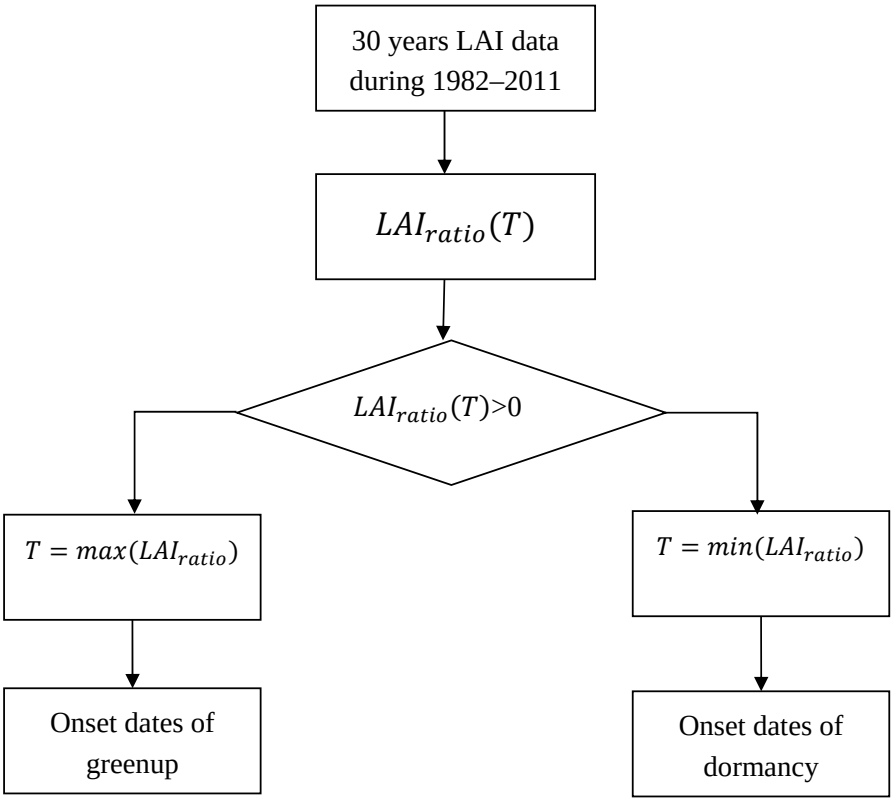

Figure 2. The approach flowchart of this study. LAI, leaf area index.

First of all, the leaf area index change ratios (LAI_{ratio}) were calculated from the series of consecutive 15-day periods from the LAI3g dataset. We calculated the leaf area index ratio for the whole study area according to the following equation:

$$LAI_{ratio}(T) = \frac{LAI(T+1) - LAI(T)}{LAI(T)} \quad (1)$$

where T is the number of the LAI image series for one year, with a 15-day interval (from 1 to 23).

The time of the maximum (minimum) LAI change ratio can be considered as the onset dates of vegetation green up(dormancy) [11,31].We firstly detected the time T with the maximum LAI_{ratio}, and then used the time T as the onset date of green-up. Likewise, we detected the time T with the minimum LAI_{ratio}, and then used the time $T + 1$ as the onset date of vegetation dormancy.

2.3.3. Mann-Kendall Trend Tests

The Mann-Kendall trend test approach is widely used in the analysis of various types of environmental data for testing monotonic trends [45,46]. The purpose of the Mann-Kendall (MK) testis to statistically assess if there is a monotonic upward or downward trend in the variable of interest over time [47]. Because the MK statistics can effectively distinguish the difference between natural variability and trend change, the MK test was used for investigating the trends of long time series of consecutive temperature observations data and leaf index data in this study.

According to the calculated MK test statistic value of long time series data in this study, the null hypothesis of no trend in the time series of consecutive temperature observations or LAI data was determined to be accepted or rejected using reference test values at the 99% confidence interval.

2.3.4. The Savitzky–Golay Filter

Satellite time series are usually noisy and discontinuous, which can lead to large uncertainties in the estimation of phenological metrics [21]. To reduce such uncertainties, these data require smoothing and gap-filling before being used in phenological studies. The Savitzky-Golay filter is one of the most commonly used filters among phonological studies [5,22,25,35].

The Savitzky–Golay (S-G) filter is a simplified least-squares-fit convolution for smoothing and computing derivatives of a set of consecutive values [48]. The S-G filter can be understood as a weighted moving average filter with weighting given as a polynomial of a certain degree. This filter can be applied to any consecutive data when the points of the data are at a fixed and uniform interval along the chosen abscissa, especially for time-series data. The general equation of the simplified least-squares convolution for time-series data smoothing include two parameters that must be determined according to the time-series data observations when the filter is applied. The first parameter is the half-width of the smoothing window. The second parameter is the degree of the smoothing polynomial. In this study, the two parameters were set as (2, 3).

2.3.5. Regression Analysis

Generally, the leaf area index of vegetation would increase firstly and then decrease gradually over the growing season. The relationship between leaf area index and the corresponding Julian day can be fitted by using Equation (2).

$$LAI = a_0 + a_1x^1 + a_2x^2 + a_3x^3 + a_4x^4 + a_5x^5 + a_6x^6 \quad (2)$$

where x is the Julian day for LAI image index. a_i ($i \in [1,\ 6]$) refers to the coefficients of sixth-degree polynomial function which can help smooth the impact of some abnormal LAI values caused from the non-vegetation effects of cloud, atmosphere, solar zenith angle, and other factors.

3. Results

3.1. Spatial Distribution of NE China Phenology

3.1.1. Phenology Derived from Temperature

Temperature variations due to differences in geographical position and elevation also mean that the phenology varies in different areas. As shown in Figure 3, the earliest SOS mainly appears in the southeastern part of study area, and the late SOS occurs at the higher latitudes of NE China area. According to the Julian calendar, the latest SOS of NE China appears later than 150 days of the year. Instead, the spatial distribution of the EOS is generally opposite to the SOS, as shown in Figure 3. The EOS day is gradually delayed from Northern NE China to the southeastern NE China area.

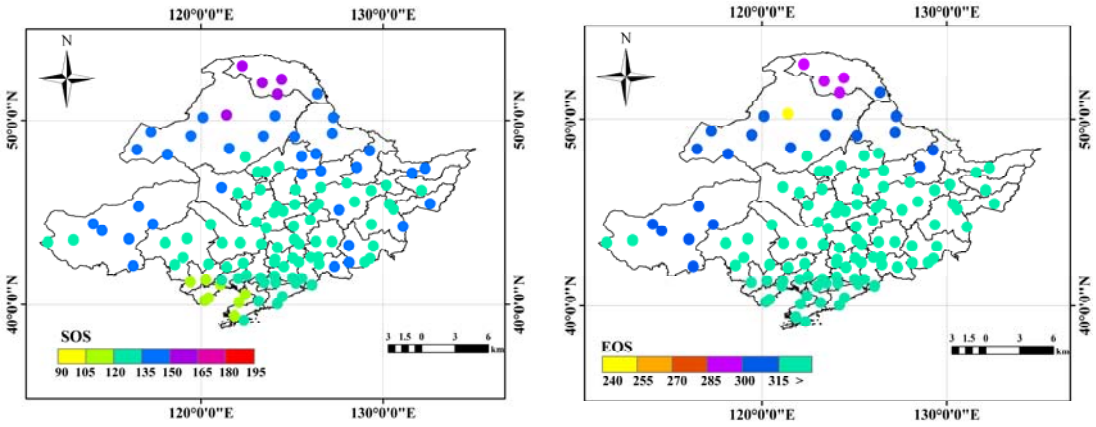

(**a**) SOS (**b**) EOS

Figure 3. The Mean annual phenology pattern of start of the growing season (SOS) and the end of the growing season (EOS) based on temperature data from the meteorological station observations. (**a**) The phenology pattern of start of the growing season (SOS); (**b**) The phenology pattern of the end of the growing season (EOS).

3.1.2. Phenology Derived from Satellite-Based LAI3g

In order to observe more details of vegetation phenology in NE China, we used the long time series of remotely sensed LAI data. In Figure 4a, we can see the earliest SOS appearing in March, which mainly occurred in the southeastern NE China area (specially in southeastern Liaoning Province). The latest SOS mainly appears in June, which mainly occurred in the western NE China area (located in Inner Mongolia) and the central NE China area (located in Changbai Mountain), which might be caused by the precipitation or the altitude.

Instead, the earliest EOS derived from LAI appears in August and mainly is distributed in the western NE China area and the mountain areas of central NE China area, which is different from the temperature-based results, and the later EOS appears September to late October, which occurred from north to south of the NE China area. Most of the latest EOSs occurred in the southern region of Liaoning Province.

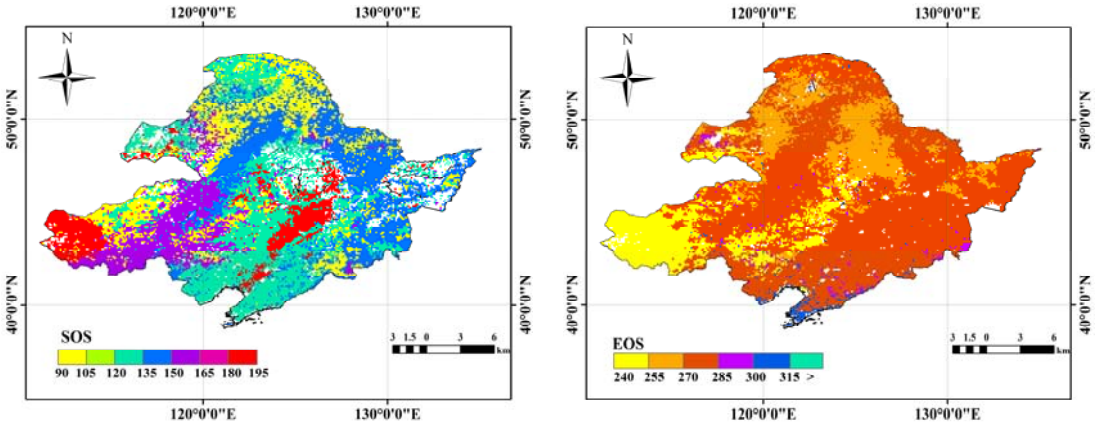

(**a**) SOS (**b**) EOS

Figure 4. The Mean annual phenology of the start of the growing season (SOS) and the end of the growing season (EOS) based on vegetation index dynamic ratio threshold. (**a**) The phenology of start of the growing season (SOS); (**b**) The phenology of the end of the growing season (EOS).

3.2. PhenologyTrends

3.2.1. Temperature-Based Phenology Trend

In order to investigate the temperature-based phenology trend, we firstly used the Mann-Kendall Trend test to identify the significant advanced trend (SAT), significant delayed trend (SDT), and nonsignificant trend (NT).

According to the statistical value of 1.96 at significance level of 0.05, trends are divided into significant advanced trend (SAT), significant delayed trend (SDT), and nonsignificant trend (NT) [22]. The results shown in Figure 5 indicate the significant advanced SOS trend can be observed in most of the study area. Instead, the nonsignificant trend (NT) appears at a small quantity of remaining meteorological sites which are distributed in northern and central parts of study area. The results of EOS are completely different from SOS (see Figure 5a,b). The significant delayed trend of EOS showed a scattered distribution at a small quantity of sites in western and central NE China.

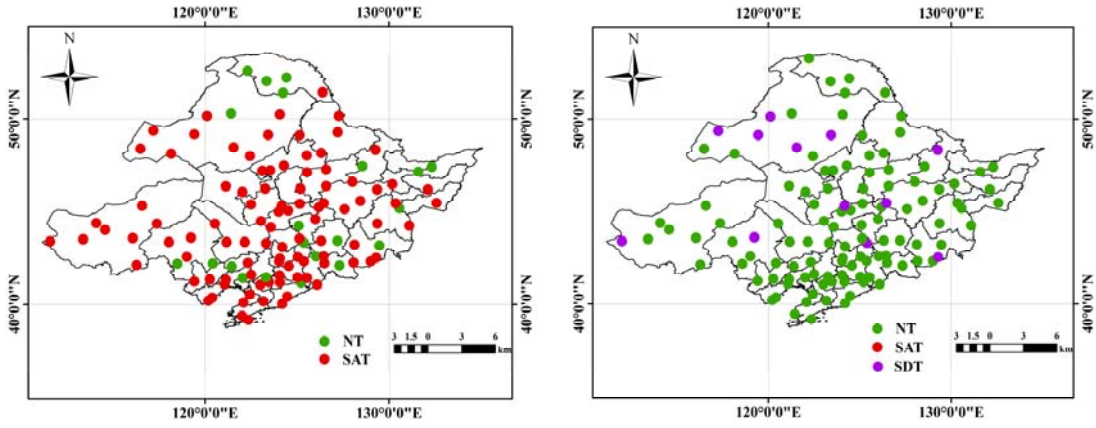

(**a**) SOS (**b**) EOS

Figure 5. Trends detections of the start of the growing season (SOS) and the end of the growing season (EOS) based on temperature data from the meteorological station observations. (**a**) The trend detection result of SOS; (**b**) The trend detection result of EOS. NT, nonsignificant trend; SAT, significant advanced trend; SDT, significant delayed trend.

3.2.2. Satellite-Derived Vegetation Phenology Trend

We also investigated the phenology trend based on the long time series SOS and EOS during the 1982–2011 period by using the Mann-Kendall Trend test approach. We respectively divided the long time series SOS and EOS into significant advanced trend (SAT), significant delayed trend (SDT), and nonsignificant trend (NT) according to the statistical value of 1.96 at significance level of 0.05. The result of satellite-based phenology trend is shown in Figure 6. However, the satellite-based phenology trend is not exactly the same as that from temperature (Figure 5).

The significant advanced SOS trend is mainly distributed in the northern and central area of NE China (including northwestern Jilin Province, northeastern Inner Mongolia, and most HeilongJiang Province and western Liaoning Province). In most parts of NE China, there is a nonsignificant SOS trend. However, other than that, there are several scattered parts showing significant delayed SOS trend in western NE China. On the contrary, significant advanced trend (SAT) of EOS derived from the LAI data is mainly distributed in a small central part of NE China, and there are some significant delayed EOSs distributed in northwestern NE China (including the northeastern Inner Mongolia and the northwestern Heilongjiang Province). Also, most of area indicates a nonsignificant EOS trend.

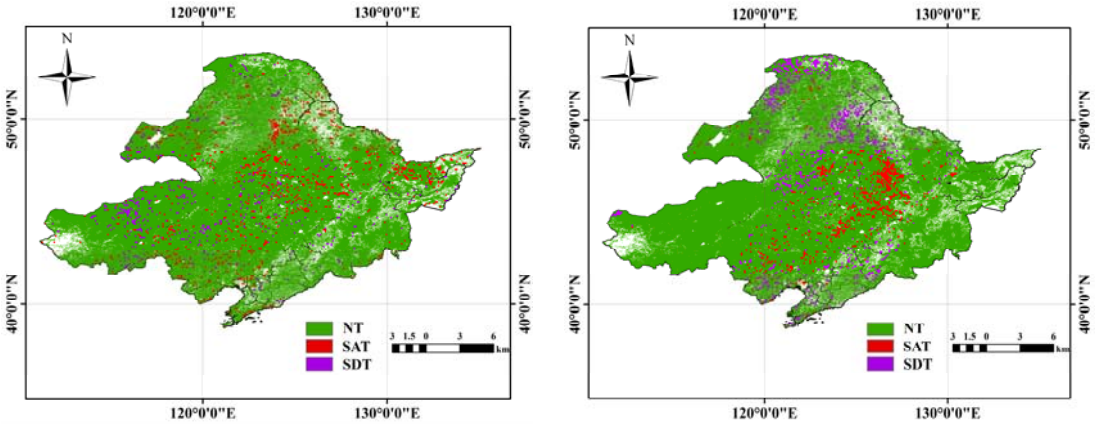

(**a**)SOS (**b**)EOS

Figure 6. Trend detections of the start of the growing season (SOS) and the end of the growing season (EOS) based on the long time series SOS and EOS derived from the long time series LAI data. (**a**) The trend detection result of SOS; (**b**) The trend detection result of EOS.

3.2.3. Comparison of Trends between Temperature-Based and Satellite-Based Phenology

Overall, there is a relatively obvious difference between temperature-based and satellite-based phenology (Figures 5 and 6). According to phenology trend investigation results, significant delayed trend (SDT) of SOS and significant advanced trend (SAT) of EOS derived from the temperature of meteorological station observations did not appear in the study area and the significant delayed trend (SDT) of EOS only distributed in parts of the meteorological stations. Most meteorological stations display the significant advanced SOS trend. On the contrary, the satellite-derived vegetation phenology trend appeared to be a nonsignificant trend (NT) in most of the study area. The 30 year phenology trend derived from long time series LAI (Figure 6) indicated that the advanced SOS and delayed EOS trends are also significant in high latitudes and the central high altitude area.

In order to understand the phenology trend change in detail, we separately calculated the 30 years phenological time series based on the temperature and LAI3g data (Figure 7a,b). Figure 7a shows the temperature-based phenological time series on the meteorological station scale. The regression results of phenology date indicate that the SOS and EOS ambiguously present an advanced and delayed linear trend, respectively, and the advanced SOS and the delayed EOS in the 118 meteorological stations changed by0.048 days year^{-1} and 0.1092 days year^{-1}, respectively.

Based on the averaged SOS and EOS derived from LAI and the corresponding LAI data, we calculated the parameters of the regression equation (Equation (2)). Then, Equation (2) can be rewritten respectively for estimating SOS and EOS phenology date. According to the equation rewritten for estimating SOS and EOS phenology dates, we calculated the phenological time series for the 30 years for the whole study area (Figure 7b). As is shown in Figure 7b, the regression results of phenology date indicate that the SOS and EOS significantly present an advanced and delayed linear trend, and the advanced SOS and the delayed EOS in the whole study area changed by 0.2593 days year^{-1} and 0.1092 days year^{-1}, respectively.

In Figure 7, the comparison result between temperature-based and satellite-based phenology time series shows that SOS derived from temperature is generally earlier than the satellite-based SOS phenology time, and the EOS derived from temperature is generally later than the satellite-based EOS phenology time.

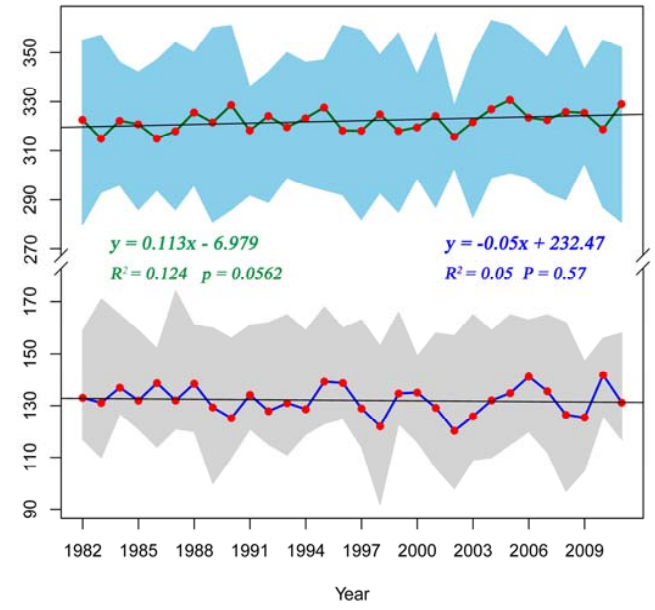

(**a**)

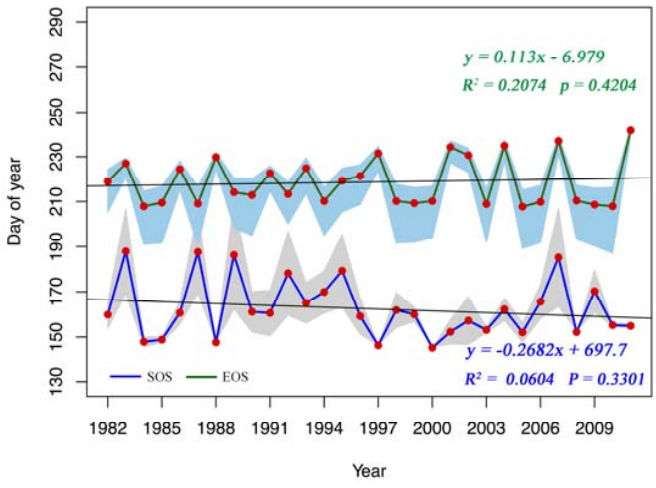

(**b**)

Figure 7. The trends of the start of the growing season (SOS) and the end of the growing season (EOS) derived from the temperature and LAI3g data during the 30 years from 1982 to 2011. (**a**) The temperature-based phenology trends at the meteorological station scale; (**b**) LAI3g-based phenology trends for the whole study area. The shadowed area means the standard deviation of phenology day.

4. Discussion

This study estimated that the satellite derived mean onset date of green-up of NE China has advanced on average by 0.2593 days year^{-1} from 1982 to 2011, and the temperature based advanced SOS of NE China changed by0.048 days year^{-1}. There is evidence across a wide range of geographic locations that the growing season has been occurring increasingly earlier in recent decades [49–51]. Numerous research studies have suggested that global warming was the primary driving force for the enhanced vegetation growth over the Northern Hemisphere [9–11,16,17,52]. The difference between temperature based and satellite based phenology trends indicates that there are otherpossible factors causing the phenology change. Additionally, different vegetation types may require different temperature thresholds to trigger the start of the growing season. Vegetation in cold environments require lower threshold temperature than that in warm conditions [53,54].

The growing season of NE China has experienced a distinct lengthening trend over the past three decades, with an approximateannual extension of 0.3685 days. The length of growing season duration profoundly impacts the interannual variability of plant growth. The measurement of phenological trends and their variability can be considerablyhelpful to the development and production of field crops, including the changes in the farming system and crop yield [55]. In accordance with global climate warming, earlier SOS and delayed EOS generally prevailed, which would be helpful for higher and more stable crop yields and improved food quality in Northeastern China. Of course, the effects of prolonged growing season might be contradictory. The longer growing season would consume more irrigated water. At the same time, the longer growing season might cause more negative impacts to human.

This study is the first to detect the phenology trends from 1982 to 2011 in the Northeast region of China. While we have achieved some research goals with this study, there are still a few points that should be addressed in the future. At the same time, the significant area in the northern part of the study area with earliest SOS based on LAI3g data could have some conflicting results, which should be discussed.

5. Conclusions

In this study, we demonstrated that the vegetation phenology derived from the satellite based LAI3g data can reflect more phenology detail from a spatio-temporal perspective than meteorological station temperature data. Based on the LAI3g data, we estimated the phenology of the Northeastern China region by using the vegetation index change ratios methods. According to the phenology result across the whole NE China area, the earliest SOS and the latest EOS mainly occurred in the southeastern NE China area. Instead, the latest SOS and the earliest EOS mainly occurred in the western NE China area (located in Inner Mongolia) and the central NE China area (located in Changbai Mountain). The satellite-based phenology can reflect the actual change in vegetation phenology of Northeastern China. However, the traditional thermal method derived from temperature cannot detect the actual vegetation phenology change in NE China, which might be caused from the difference of the changes in water availability and temperature.

The average trends of SOS in the northern and central areas of NE China show the significant advanced phenology trend. Meanwhile, there is some significant delayed EOS with a scattered distributed in northwestern NE China. However, most parts of NE China did not show a significant phenology trend.

Based on temperature and long time-series LAI3g data during the period of 1982–2011, we estimated that the growing season duration of vegetation in Northeastern China region has a relatively significant lengthened trend. The results of this study strongly support the view that lengthening of growing season duration at the northern high latitudes appeared in recent decades owing to global warming. The difference of phenology between the temperature based traditional thermal method and satellite-based vegetation index metric reported in this study can result in significant results in interpreting the possible influence of climate change on vegetation phenology change in some important

regions. This finding not only underlines the importance of temperature for vegetation phenology, but also suggests that the possible influence on vegetation phenology should be included in future phonological models.

Acknowledgments: The authors would like to thank the three anonymous reviewers whose comments significantly improved this manuscript. This work was supported by the Key Programs of the Chinese Academy of Sciences (Grant No.KZZD-EW-TZ-17) and Sciences Technology Service project of Chinese Academy of Sciences(2016, Grant No. KFJ-SW-STS-167). This study was also partly funded by the National Natural Science Foundation of China (2016, Grant No.41601478), National Key R&D Program (2016YFC0500103) and the open fund of State Key Laboratory of Resources and Environment Information System (LREIS, 2016).

Author Contributions: The analysis was performed by Xiliang Ni, JianfengXie, and Yuke Zhou. All authors contributed with ideas, writing, and discussions.

Conflicts of Interest: The authors declare no conflict of interest.

References

1. Post, E.; Forchhammer, M.C.; Bret-Harte, M.S.; Callaghan, T.V.; Christensen, T.R.; Elberling, B.; Ims, R.A. Ecological dynamics across the arctic associated with recent climate change. *Science* **2009**, *325*, 1355–1358. [CrossRef] [PubMed]
2. Tao, F.; Zhang, S.; Zhang, Z. Changes in rice disasters across China in recent decades and the meteorological and agronomic causes. *Reg. Environ. Chang.* **2013**, *13*, 743–759. [CrossRef]
3. Schwartz, M.D. Advancing to full bloom: Planning phonological research for the 21st century. *Int. J. Biometeorol.* **1999**, *42*, 113–118. [CrossRef]
4. White, M.A.; Thornton, P.E.; Running, S.W. Acontinental phenology model for monitoring vegetation responses to inter annual climatic variability. *Glob. Biogeochem. Cycles* **1997**, *11*, 217–234. [CrossRef]
5. Piao, S.L.; Friedlingstein, P.; Ciais, P.; Viovy, N.; Demarty, J. Growing season extension and its effects on terrestrial carbon flar over the last two decades. *Glob. Biogeochem. Cycles* **2007**, *21*, GB3018. [CrossRef]
6. Myneni, R.B.; Keeling, C.D.; Tucker, C.J.; Asrar, G.; Nemani, R.R. Increased plant growth in the northern high latitudes from 1981–1991. *Nature* **1997**, *386*, 698–702. [CrossRef]
7. Peñuelas, J.; Rutishauser, T.; Filella, I. Phenology feedbacks on climate change. *Science* **2009**, *324*, 887–888. [CrossRef] [PubMed]
8. Peckham, S.D.; Ahl, D.E.; Serbin, S.P.; Gower, S.T. Fire induced changes in green up and leaf maturity of the Canadian boreal forest. *Remote Sens. Environ.* **2008**, *112*, 3594–3603. [CrossRef]
9. Piao, S.; Fang, J.; Zhou, L.; Guo, Q.; Henderson, M.; Ji, W.; Tao, S. Inter annual variations of monthly and seasonal Normalized Difference Vegetation Index (NDVI) in China from 1982 to 1999. *J. Geophys. Res.: Atmos.* **2003**, *108*, 4401. [CrossRef]
10. Shen, M.G.; Tang, Y.H.; Chen, J.; Yang, W. Specification of thermal growing season in temperate China from 1960 to 2009. *Clim. Chang.* **2012**, *114*, 783–798. [CrossRef]
11. Piao, S.L.; Fang, J.Y.; Zhou, L.M.; Ciais, P.; Zhu, B. Variations in satellite derived phenology in China's temperate vegetation. *Glob. Chang. Biol.* **2006**, *12*, 672–685. [CrossRef]
12. Ahl, D.E.; Gower, S.T.; Burrows, S.N.; Shabanov, N.V.; Myneni, R.B.; Knyazikhin, Y. Monitoring spring canopy phenology of a deciduous broadleaf forest using MODIS. *Remote Sens. Environ.* **2006**, *104*, 88–95. [CrossRef]
13. Piao, S.; Sitch, S.; Ciais, P.; Piao, S.; Sitch, S.; Ciais, P.; Friedlingstein, P.; Peylin, P.; Wang, X.; Ahlström, A.L.; et al. Evaluation of terrestrial carbon cycle models for their response to climate variability and to CO_2 trends. *Glob. Chang. Biol.* **2013**, *19*, 2117–2132. [CrossRef] [PubMed]
14. Fisher, J.I.; Mustard, J.F.; Vadeboncoeur, M.A. Green leaf phenology at landsat resolution: Scaling from the field to the satellite. *Remote Sens. Environ.* **2006**, *100*, 265–279. [CrossRef]
15. Tateishi, R.; Ebata, M. Analysis of phenological change patterns using 1982–2000 advanced very high resolution radiometer (AVHRR) data. *Int. J. Remote Sens.* **2004**, *25*, 2287–2300. [CrossRef]
16. Myneni, R.B.; Yang, W.; Nemani, R.R.; Huete, A.R.; Dickinson, R.E.; Knyazikhin, Y.; Hashimoto, H. Large seasonal swings in leaf area of Amazon rainforests. *Proc. Natl. Acad. Sci. USA* **2007**, *104*, 4820–4823. [CrossRef] [PubMed]

17. Mao, J.; Shi, X.; Thornton, P.E.; Hoffman, F.M.; Zhu, Z.; Myneni, R.B. Global latitudinal-asymmetric vegetation growth trends and their driving mechanisms: 1982–2009. *Remote Sens.* **2013**, *5*, 1484–1497. [CrossRef]
18. Li, M.; Qu, J.J.; Hao, X. Investigating phonological changes using MODIS vegetation in deciduous Broadleaf forest over continental U.S. during 2000–2008. *Ecol. Inf.* **2010**, *5*, 410–417. [CrossRef]
19. Atkinson, P.M.; Jeganathan, C.; Dash, J.; Atzberger, C. Inter-comparison of four models for smoothing satellite sensor time-series data to estimate vegetation phenology. *Remote Sens. Environ.* **2012**, *123*, 400–417. [CrossRef]
20. Kandasamy, S.; Baret, F.; Verger, A.; Neveux, P.; Weiss, M.A. Comparison of methods for smoothing and gap filling time series of remote sensing observations Application to MODIS LAI products. *Biogeosciences* **2013**, *10*, 4055–4071. [CrossRef]
21. Kandasamy, S.; Fernandes, R. An approach for evaluating the impact of gaps and measurement errors on satellite land surface phenology algorithms: Application to 20 year NOAA AVHRR data over Canada. *Remote Sens. Environ.* **2015**, *164*, 114–129. [CrossRef]
22. Zhu, Z.; Piao, S.; Myneni, R.B.; Huang, M.; Zeng, Z.; Canadell, J.G.; Cao, C. Greening of the Earth and its Drivers. *Nat. Clim. Chang.* **2016**, *6*, 791–795. [CrossRef]
23. Anav, A.; Friedlingstein, P.; Kidston, M.; Bopp, L.; Ciais, P.; Cox, P.; Zhu, Z. Evaluating the land and ocean components of the global carbon cycle in the CMIP5 earth system models. *J. Clim.* **2013**, *26*, 6801–6843. [CrossRef]
24. Cook, B.I.; Pau, S. A global assessment of long-term greening and browning trends in pasture lands using the GIMMS LAI3g dataset. *Remote Sens.* **2013**, *5*, 2492–2512. [CrossRef]
25. Piao, S.; Fang, J.; Ciais, P.; Huang, Y.; Sitch, S.; Wang, T. The carbon balance of terrestrial ecosystems in China. *Nature* **2009**, *458*, 1009–1013. [CrossRef] [PubMed]
26. Busetto, L.; Colombo, R.; Migliavacca, M.; Cremonese, E.; Meroni, M.; Galvagno, M.; Rossini, M.; Siniscalco, C.; DiCella, U.M.; Pari, E. Remote sensing of larch phonological cycle and analysis of relationships with climate in the Alpine region. *Glob. Chang. Biol.* **2010**, *16*, 2504–2517.
27. Xu, L; Myneni, R.B.; Chapin, F.S., III; Pinzon, J.E.; Tucker, C.J.; Zhu, Z.; Bi, J.; Ciais, P.; Tømmervik, H.; Euskirchen, E.S.; et al. Temperature and vegetation seasonality diminishment over northern lands. *Nat. Clim. Chang.* **2013**, *3*, 581–586. [CrossRef]
28. Zhu, Z.; Bi, J.; Pan, Y.; Ganguly, S.; Anav, A.; Xu, L.; Myneni, R.B. Global data sets of vegetation leaf area index(LAI) 3g and Fraction of Photosynthetically Active Radiation (FPAR) 3g derived from Global Inventory Modeling and Mapping Studies (GIMMS) Normalized Difference Vegetation Index (NDVI3g) for the period 1981 to 2011. *Remote Sens.* **2013**, *5*, 927–948.
29. Choi, S.; Ni, X.; Shi, Y.; Ganguly, S.; Zhang, G.; Duong, H.V.; Lefsky, M.A.; Simard, M.; Saatchi, S.S.; Lee, S. Allometric scaling and resource limitations model of tree heights: Part 2. Site based testing of the model. *Remote Sens.* **2013**, *5*, 202–223. [CrossRef]
30. Ni, X.; Park, T.; Choi, S.; Shi, Y.; Cao, C.; Wang, X.; Lefsky, M.A.; Simard, M.; Myneni, R.B. Allometric scaling and resource limitations model of tree heights: Part 3. Model optimization and testing over continental China. *Remote Sens.* **2014**, *6*, 3533–3553. [CrossRef]
31. Ni, X.; Zhou, Y.; Cao, C.; Wang, X.; Shi, Y.; Park, T.; Choi, S.; Myneni, R.B. Mapping Forest Canopy Height over Continental China Using Multi-Source Remote Sensing Data. *Remote Sens.* **2015**, *7*, 8436–8452. [CrossRef]
32. Friedl, M.A.; Sulla-Menashe, D.; Tan, B.; Schneider, A.; Ramankutty, N.; Sibley, A.; Huang, X. MODIS Collection 5 global land cover: Algorithm refinements and characterization of new datasets. *Remote Sens. Environ.* **2010**, *114*, 168–182. [CrossRef]
33. Jiang, F.Q.; Hu, R.J.; Zhang, Y.W.; Li, X.M.; Tong, L. Variations and trends of onset, cessation and length of climatic growing season over Xinjiang, NW China. *Theor. Appl. Climatol.* **2011**, *106*, 449–458. [CrossRef]
34. Wang, Y.; Shen, Y.; Sun, F.; Chen, Y. Evaluating the vegetation growing season changes in the arid region of northwestern China. *Theor. Appl. Climatol.* **2014**, *118*, 569. [CrossRef]
35. Jong, R.; Bruin, S.; Wit, A.; Schaepman, M.E.; Dent, D.L. Analysis of monotonic greening and browning trends from global NDVI time-series. *Remote Sens. Environ.* **2011**, *115*, 692–702.
36. Brown, M.E.; De Beurs, K.; Vrieling, A. The response of African land surface phenology to large scale climate oscillations. *Remote Sens. Environ.* **2010**, *114*, 2286–2296. [CrossRef]
37. Yu, H.Y.; Luedeling, E.; Xu, J.C. Winter and spring warming result in delayed spring phenology on the Tibetan Plateau. *Proc. Natl. Acad. Sci. USA* **2010**, *107*, 22151–22156. [CrossRef] [PubMed]

38. Kaduk, J.; Heimann, M. A prognostic phenology scheme for global terrestrial carbon cycle models. *Clim. Res.* **1996**, *6*, 1–19. [CrossRef]
39. Moulin, S.; Kergoat, L.; Viovy, N.; Dedieu, G. Global-scale assessment of vegetation phenology using NOAA/AVHRR satellite measurements. *J. Clim.* **1997**, *10*, 1154–1170. [CrossRef]
40. Lee, R.; Yu, F.; Price, K.P. Evaluating vegetation phonological patterns in Inner Mongolia using NDVI time-series analysis. *Int. J. Remote Sens.* **2002**, *23*, 2505–2512. [CrossRef]
41. Yu, F.; Price, K.P.; Ellis, J.; Shi, P. Response of seasonal vegetation development to climatic variations in eastern central Asia. *Remote Sens. Environ.* **2003**, *87*, 42–54. [CrossRef]
42. Zhang, X.; Friedl, M.A.; Scahaaf, C.B.; Strahler, A.H.; Hodges, J.C.; Gao, F.; Huete, A. Monitoring vegetation phenology using MODIS. *Remote Sens. Environ.* **2003**, *84*, 471–475. [CrossRef]
43. Zhang, X.Y.; Friedl, M.A.; Schaaf, C.B.; Strahler, A.H. Climate controls on vegetation phonological patterns in northern mid-and high latitudes inferred from MODIS data. *Glob. Chang. Biol.* **2004**, *10*, 1133–1145. [CrossRef]
44. Hipel, K.W.; McLeod, A.I. *Time Series Modelling of Water Resources and Environmental Systems*; Elsevier: Amsterdam, The Netherlands, 1994.
45. McLeod, A.I.; Hipel, K.W.; Bodo, B.A. Trend analysis methodology for water quality time series. *Environmetrics* **1990**, *2*, 169–200. [CrossRef]
46. Mann, H.B. Non-parametric tests against trend. *Econometrica* **1945**, *13*, 163–171. [CrossRef]
47. Penuelas, J.; Filella, I.; Comas, P. Changed plant and animal life cycles from 1952 to 2000 in the Mediterranean region. *Glob. Chang. Biol.* **2002**, *8*, 531–544. [CrossRef]
48. Jeong, S.-J.; Ho, C.-H.; Gim, H.-J.; Brown, M.E. Phenology shifts at start vs. end of growing season in temperate vegetation over the Northern Hemisphere for the period 1982–2008. *Glob. Chang. Biol.* **2011**, *17*, 2385–2399. [CrossRef]
49. Hegerl, G.C.; Hoegh-Guldberg, O.; Casassa, G.; Hoerling, M.P.; Kovats, R.S.; Parmesan, C.; Stott, P.A. Good Practice Guidance Paper on Detection and Attribution Related to Anthropogenic Climate Change. In *Meeting Report of the Intergovernmental Panel on Climate Change Expert Meeting on Detection and Attribution of Anthropogenic Climate Change*; IPCC Working Group I Technical Support Unit, University of Bern: Bern, Switzerland, 2010.
50. Peng, S.; Chen, A.; Xu, L.; Cao, C.; Fang, J.; Myneni, R.B.; Piao, S. Recent change of vegetation growth trend in China. *Environ. Res. Lett.* **2011**, *6*, 044027. [CrossRef]
51. Richardson, A.D; Keenan, T.F; Migliavacca, M; Ryu, Y; Sonnentag, O; Toomey, M. Climate change, phenology, and phonological control of vegetation feedbacks to the climate system. *Agric. For. Meteorol.* **2013**, *169*, 156–173. [CrossRef]
52. Jobbagy, E.G.; Sala, O.E.; Paruelo, J.M. Patterns and controls of primary production in the Patagonian steppe: A remote sensing approach. *Ecology* **2002**, *83*, 307–319.
53. Chen, B.; Zhang, X.; Tao, J.; Wu, J.; Wang, J.; Shi, P.; Yu, C. The impact of climate change and anthropogenic activities on alpine grassland over the Qinghai-Tibet Plateau. *Agric. For. Meteorol.* **2014**, *189*, 11–18. [CrossRef]
54. Pan, Y.; Birdsey, R.A.; Fang, J.; Houghton, R.; Kauppi, P.E.; Kurz, W.A.; Ciais, P. A large and persistent carbon sink in the world's forests. *Science* **2011**, *333*, 988–993. [CrossRef] [PubMed]
55. Sacks, W.J.; Kucharik, C.J. Crop management and phenology trends in the US Corn Belt: Impacts on yields, evapotranspiration and energy balance. *Agric. For. Meteorol.* **2011**, *151*, 882–894. [CrossRef]